

*The final publication is available at Springer via <http://dx.doi.org/10.1007/s00216-011-5318-3>  
Analytical and Bioanalytical Chemistry, 2012, Volume 402, pp 1759-1771.*

## **Functionalized gold nanoparticles for the ultrasensitive DNA detection**

Laura Maria Zanoli,<sup>1</sup> Roberta D'Agata,<sup>2</sup> Giuseppe Spoto<sup>2,3\*</sup>

<sup>1</sup> Scuola Superiore di Catania, c/o Dipartimento di Scienze Chimiche, Università di Catania, Viale Andrea Doria 6, Catania, Italy

<sup>2</sup> Dipartimento di Scienze Chimiche, Università di Catania, Viale Andrea Doria 6, I-95125 Catania, Italy

<sup>3</sup> Istituto Biostrutture e Bioimmagini, CNR, Viale A. Doria 6, Catania, Italy

Correspondence to:

Giuseppe Spoto, Dipartimento di Scienze Chimiche, Università di Catania, Viale Andrea Doria 6, 95125, Catania, Italy, e-mail: [gspoto@unict.it](mailto:gspoto@unict.it)

### **Keywords**

DNA detection, gold nanoparticles, PCR-free, optical detection, electrochemical detection, SPR, QCM, scanometric detection

## **Abstract**

A major challenge in the area of DNA detection is the development of rapid methods that do not require the polymerase chain reaction (PCR) amplification of the genetic sample. The PCR amplification step increases the cost of the assay, the complexity of the detection and the quantity of DNA required for the assay. In this perspective, methods able to perform DNA analyses with ultrasensitivity have been recently investigated with the aim to develop new PCR-free detection protocols. Functionalized gold nanoparticles have played a central role in the development of such methods. Here possibilities offered by functionalized gold nanoparticle in the ultrasensitive detection of DNA are discussed. The different functionalization protocols available for gold nanoparticles and the principal DNA detection methods able to detect DNA at the femtomolar-attomolar level are presented.

## **Introduction**

Gold has been the first metal transformed into a colloidal state. The “beautiful ruby fluid” formed upon reduction of aqueous gold chloride with phosphorous dissolved in carbon disulfide was first described by Michael Faraday in 1857<sup>1</sup> but it was only until 1908 that the colour effects connected with colloidal gold nanoparticles were rationalized by Gustav Mie.<sup>2</sup> The intense red color of AuNPs is due to the interaction of incident light with a collective oscillation of free electrons in the particles known as localized surface plasmon resonance. AuNPs with different diameters in the range of about 10-100 nm or AuNP aggregation produces color changes from red to blue. Today, gold nanoparticles (AuNPs) are synthesized by using different methods and have been the focus of extensive research activities.<sup>3,4</sup> AuNP surface and core properties can be engineered for a wide range of bioanalytical applications<sup>5,6</sup> in which biomolecules and nanoparticles typically meet at the same nanometer length scale.<sup>7</sup> DNA biomolecules are particularly suitable for applications in nanobiotechnology<sup>8,9</sup> and a number of different fields have benefitted from such applications. In

particular, the development of innovative methods for DNA detection is a research field which has mostly benefitted from DNA nanobiotechnology.

The growing interest in DNA detection, associated with the need for highly parallel and miniaturized assays, has prompted the development of sensitive and low cost technologies able to use the vast amount of information made available by genome sequencing.<sup>10</sup> Traditional DNA sensing technologies rely on a combination of amplification of the target DNA sequence by polymerase chain reaction (PCR) and optical detection based on the use of fluorophore labels. However, several major drawbacks still remain, which are associated with the need for expensive reagents and pitfalls due to contamination or matrix effects.<sup>11</sup> In particular, PCR involves time consuming thermal cycles and is subject to severe contamination problems and for these reasons a major challenge for rapid and reliable DNA analysis appears to be the development of ultrasensitive rapid and multiplexed methods able to perform PCR-free DNA analyses. In fact, sensitivity as high as 1 pM helps in avoiding the PCR amplification step. Metallic nanoparticles have been shown to greatly enhance sensitivity in DNA detection when used for labelling purposes but also as modifiers of transducers.<sup>12,13</sup>

AuNPs are the most widely used nanostructures for DNA detection for several reasons: *i*) simple synthetic procedures are required in order to obtain AuNPs having pretty well controlled diameters, shapes and optical properties, *ii*) AuNPs possess extremely high extinction coefficients ( $2.7 \times 10^8 \text{ M}^{-1} \text{ cm}^{-1}$  at  $\sim 520 \text{ nm}$  for 13 nm spherical AuNPs),<sup>14</sup> thus slight aggregation may result in intense color changes, *iii*) the nanoparticle large surface area allows the load of hundreds of capture probe DNAs, meanwhile the three dimensional assembly of the probe lowers the steric hindrance and favours target-probe hybridization.

In this review, we will summarize recent advances in DNA biosensing strategies using functionalized AuNPs. While a few excellent reviews have given comprehensive summaries of the updated processes involving DNA sensors and DNA microarrays,<sup>4,15,16,17,18</sup> here we will focus on some recent advances on the ultrasensitive detection of DNA.

## **AuNPs for the ultrasensitive DNA detection**

Applications of AuNPs in DNA detection are strongly related to nanoparticle chemical and physical properties. A proper selection of synthetic procedures and following chemical and biological modifications of the synthesized AuNPs allow the tuning of the relevant properties of the nanoparticles.<sup>12</sup>

A detailed discussion of the different synthetic strategies useful in obtaining AuNPs having different dimensions and shapes is out of the scope of the present review.<sup>19,20,21</sup> However, it is worth mentioning that the most widely adopted synthetic procedures involve the chemical or electrochemical reduction of Au(III) precursor compounds in the presence of a capping agent. The classic Turkevich-Frens method<sup>22</sup> uses citrate ions as the capping agent in order to electrostatically stabilize nanoparticles against aggregation. The AuNP size (between 10 and 147 nm) can be controlled by the ratio between the reducing/capping citrate agent and Au(III) precursor derivative (the hydrogen/sodium tetrachloroaurate (III)).<sup>23</sup> The Turkevich-Frens method is used frequently even now since the rather loose shell of citrates on the particle-surfaces is easily replaced by other desired ligands with valuable functions. Once prepared, AuNPs are stable for long periods and, because they are generally employed at very low concentrations, they are cheap even though the material from which they are made is proverbially expensive.<sup>24</sup>

Monodisperse AuNPs are red-coloured and exhibit a relatively narrow surface plasmon absorption band at 520 nm.<sup>25</sup> In contrast, aggregated AuNPs appear blue-purple in colour, corresponding to a characteristic red shift of the surface plasmon resonance. AuNPs are unique because their nanometer size gives rise to a high reactivity and physical properties (electrical, optical, catalytic and magnetic) can be easily tailored by chemically modifying their surfaces. The fascinating size- and shape-dependent optical properties make AuNPs ideal nanomaterials for sensing applications.<sup>26,27</sup>

The ultimate goal of AuNPs surface modification with biomolecular systems is to preserve the properties of both the AuNP as well as the bound molecule. In fact, the surface bound biomolecule

must be stable and able to retain its biorecognition properties and AuNPs must retain their unique properties such as strong surface plasmon absorption bands and light scattering.

Functionalization of AuNPs with biomolecular systems has only been carried out with a limited number of the strategies (**Fig. 1**): *i*) ligand-like binding to the surface of the AuNP; the biomolecules are simply adsorbed either directly to the AuNP surface or to the shell of stabilizing ions or molecules around the nanoparticles; *ii*) electrostatic adsorption of positively charged molecules to negatively charged AuNPs; through electrostatic interactions between biological molecules that are oppositely charged to the nanoparticles; *iii*) covalent binding between the biological molecule and the stabilizing shell around the AuNP; *iv*) affinity-based binding.

### **DNA-functionalized AuNPs**

After the milestone work from Mirkin's group<sup>28</sup> that in 1996 described the first colorimetric DNA sensor using functionalized AuNPs, DNA functionalized AuNPs have become popular sensing materials for DNA detection. Oligonucleotides (ODN) functionalized AuNP probes exhibit sharper melting transitions and higher melting temperatures than the corresponding fluorophores labelled ODN.<sup>29,30</sup> These unique hybridization properties enable a remarkable sequence specificity that allows an easier detection of single-base mismatches, deletions or insertions.<sup>31</sup>

ODN functionalization of AuNPs is mostly obtained through covalent binding or electrostatic interaction.<sup>32</sup> The quasi-covalent binding of thiol groups to Au surfaces is largely used to immobilize up to several hundred of thiol-modified ODN on a single AuNP. The ODN density on the AuNPs surface can be influenced by adjusting the excess ratio or by dilution with other ligands, e.g. short oligomers.<sup>33</sup> The method produces a stable immobilization of ODN on the AuNP surface and is relatively higher cost-wise when compared to other immobilization procedures. Unfortunately, even under optimized conditions<sup>34</sup> the binding of thiol-modified ODN to nanoparticles does not occur quantitatively. Moreover, no easy direct synthesis to obtain nanoparticles with an exact ODN-molecule-to-particle ratio exists; if thiol-modified ODN and

nanoparticles are mixed in a 1:1 ratio, a stoichiometric distribution will always be obtained. This means that AuNPs that are bioconjugated with unmodified and modified ODN may coexist affecting the sensitivity and reproducibility of the assays.

On the other hand, modification of AuNPs through electrostatic interaction<sup>25</sup> between ODN bases and the AuNPs surface is quite simple and cheap. However, the achieved ODN binding is not as stable as the covalent binding particularly under high ionic-strength conditions. The conformation of ODN which were electrostatically adsorbed on the AuNP surface represents another important issue to be considered. An inconvenient conformation is expected to affect the hybridization efficiency of nanoparticle immobilized ODNs. Some experimental procedures have been described in order to obtain alkanethiol-ODN molecules in a standing configuration on the surface of gold nanoparticles.<sup>35</sup>

Achieving a balance between ODN surface coverage, particle stability, and hybridization efficiency is important to obtain functionalized AuNPs to be used for sensing purposes. Coverage must be high enough to stabilize particles, yet low enough so that a high percentage of the strands are accessible for hybridization with ODN in solution. A proper surface coverage can be obtained by considering that changing salt conditions during the functionalization process induces higher loading of DNA strands due to reduced electrostatic repulsion between the negatively charged oligonucleotide strands on the nanoparticle surface.<sup>36</sup> The use of oligonucleotide spacer segments helps to reduce electrostatic and steric interactions between surface-bound ODNs and incoming complementary DNA strands involved in hybridization. Finally, co-adsorbed diluent strands can be used to control the number of hybridization events that can occur at each nanoparticle.

Besides the ligand-like direct binding of ODN to the nanoparticle surface, conjugation chemistry can also be employed to covalently bind ODN to functional groups available on the nanoparticle surface. With this purpose 1-ethyl-3-(3-dimethyl-aminopropyl)carbodiimide (EDC) chemistry is useful to bind amino-functionalized ODN to AuNPs with carboxylic groups<sup>37</sup> while maleimide groups on the AuNPs surfaces are used for thiol-modified ODN.<sup>38</sup>

Streptavidin-functionalized AuNPs have been used for the affinity binding of biotinylated ODNs.<sup>39,40</sup> The method takes advantage of both the stability of the ODN functionalization as well as the commercial availability of streptavidin-functionalized AuNPs.

### **DNA analogues-functionalized AuNPs**

DNA analogues such as peptide nucleic acids (PNAs), molecular beacons (MBs), hairpin oligonucleotides (HO) and DNAzymes have been used to functionalize AuNPs with the aim to extend the nanoparticle-based detection capabilities.<sup>26</sup>

PNAs are DNA analogues in which the negatively phosphate deoxyribose backbone is replaced by a neutral N-(2-aminoethyl)glycine linkage.<sup>41</sup> The thermal stability of the PNA/DNA duplexes is strongly affected by imperfect matches. This property is responsible for the remarkable discrimination between perfect matches and mismatches offered by PNA probes and made them so attractive as oligonucleotide recognition elements in biosensor technology.<sup>42</sup> PNAs were first used to functionalize AuNPs in 2003.<sup>43</sup> Since then difficulties encountered in conjugating standard PNA structures to nanoparticles were highlighted. PNA modification of AuNPs requires the use of unconventional PNA motifs that can be obtained by replacing glycine units of the polyamide backbone with other aminoacids.<sup>44</sup> Because of PNA's neutrality, the introduction of charge through basic or acidic residues at the polymer termini can dramatically affect the electrostatic surface properties of the modified AuNPs and represents a way to control assembly rate and aggregate size. The assembly of PNA-modified AuNPs is generally slower and results in smaller red-shifts, indicating the formation of smaller aggregates than the assembly of pure DNA-modified AuNPs.

PNA-AuNPs conjugates have been shown to be useful in discriminating single-base mismatches and detecting target sequences in the presence of a nonspecific background. In fact, the superior base pair mismatch selectivity of PNAs<sup>45</sup> is further enhanced on AuNPs surface and the colloidal stability increases significantly upon DNA hybridization.

PNAs neutral charge have also been found to play a role in the development of colorimetric DNA detection methods exploiting the unmodified citrate-protected AuNP aggregation process.<sup>46,47</sup> The use of neutral PNAs as the probe induces an immediate AuNPs aggregation in the absence of the complementary DNA strand and offers opportunities for more cost and time effective assay development.

MBs are single-stranded nucleic acid molecules that possess an hairpin structure. The loop portion of the hairpin structure is the probe sequence complementary to the target. The stem region is formed by the annealing of two complementary short sequences placed on either end of the strand. These two sequences are unrelated to the target. A fluorophore is introduced to one end of the strand while a quencher is present at the other end. The stem-and-loop structure of the beacon is so that the two moieties are kept in close proximity to each other and the fluorescence of the reporter is thus quenched.<sup>48</sup> When the probe encounters the target sequence, the loop portion of the hairpin tends to hybridize with it. As a consequence of the hairpin conformational change caused by the MB-target hybridization, the reporter is no longer in close proximity to the quencher and it emits a fluorescent signal when irradiated by the corresponding excitation wavelength.

MBs to be used to functionalize AuNPs do not require a stem in their structure as a consequence of the efficient quenching of the fluorophore caused by the non radiative energy transfer to the gold nanoparticle surface.<sup>49,50</sup> Upon target binding the MB conformational change separates the fluorophore from the particle surface and a fluorescence signal is generated. The MB-AuNPs method has been shown to allow the detection of single-base mutations more efficiently than conventional MB.

Simple hairpin oligonucleotides (HO) have also been used to modify AuNPs.<sup>51</sup> In particular, thiol-modified HO carrying a biotin unit at the 3'-end has been self-assembled on the AuNP surface. The hairpin structure of HO and the presence of deoxyadenosine triphosphate (dATP) as blockers embed the biotin groups on the AuNP surface and make it inactive. The assembled blockers contribute to reduce the nonspecific adsorption of HO-AuNPs and also to maintain the orientation



of HO probes on the gold surface thus providing a high DNA hybridization efficiency. The hybridization reactions between the target DNA sequence and the loop portion of HO on the AuNP surface forms a double stranded structure and opens the stem of the HO thus pulling the biotin away from the AuNP surface. The hybridized complex was shown to be able to react with streptavidin preimmobilized on lateral flow strips. The exploited AuNPs surface modification allows reducing non specific adsorption when compared to MB-AuNPs and provide lower signal background and higher selectivity in detecting target species.

Other possibilities in DNA detection are offered by DNAzyme-functionalized Au-NPs. DNAzymes are DNA molecules with enzyme-like catalytic activity.<sup>52</sup> The DNAzyme catalytic activity has been used for the amplified chemiluminescence detection of DNA. In fact, the DNAzyme stimulates, in the presence of hemin, H<sub>2</sub>O<sub>2</sub>, and luminol, the generation of chemiluminescence.<sup>53</sup>

### **Silver-enhanced gold nanoparticles**

Detection based on the nanoparticle colour may not be sensitive enough due to the tiny amount of material present unless the particles are in proximity.<sup>54</sup> The sensitivity of detection in the case of AuNPs probes can be increased by using the electroless silver enhancement procedure<sup>55</sup> that allows the silver deposition on AuNPs. In this technique, colloidal metal particles act as catalysts to reduce Ag<sup>+</sup> ions to metallic silver in the presence of a reducing agent. Silver amplification is particularly useful for particles that are only a few nanometers in diameter, while larger particles (>40 nm) have a sufficiently large extinction coefficient that their scattered light can be detected efficiently without the benefit of silver enhancement. In this case, the colour of the scattered light is a function of the particle size,<sup>56</sup> allowing the design of multiple colour labeling systems for array applications.<sup>57</sup>

The advantages offered by silver enhancement have allowed the development of commercially available platforms able to directly detect SNP from unamplified human genomic DNA.<sup>58,59,60</sup> Additionally, DNA-modified nanoparticles were shown to detect zeptomolar target sequences in a homogeneous colorimetric assay.<sup>61</sup>

## Ultrasensitive DNA detection

A major challenge in the area of DNA detection is the development of rapid and multiplexed methods that do not require PCR amplification of the DNA because it entails additional steps in sample pre-treatment, is time consuming and requires expensive reagents. In this perspective, PCR-free approaches allowing for DNA analyses with high-throughput and ultrasensitivity (1 pM sensitivity must be reached for the detection of unamplified DNA) have been proposed. Another important issue is the development of analytical devices which rely on a small sample amount enabling the analysis of non-amplified genomic DNA. A number of analytical techniques have been proposed to date which exploit the signal-enhancement power of AuNPs to reach the goal of the ultrasensitive detection.

In this review, only selected papers are cited in which sensitivity in the femtomolar-zeptomolar concentration range is discussed. In fact, a sensitivity reaching at least the femtomolar level is required for PCR-free clinical applications.<sup>62</sup> Few exceptions are included with a sensitivity in the pM range because they are associated with essential advantages such as the simplicity of the detection scheme and the use of innovative strategies. Table 1 summarizes working principles and performances of the discussed ultrasensitive DNA detection methods.

The most widely used DNA detection approaches relying on functionalized AuNPs exploit<sup>6</sup>: *i*) the AuNPs colour change upon nanoparticle aggregation (colorimetric detection). The best characterized example uses ODN functionalized AuNPs capable of specifically hybridize to the complementary target for the detection of specific DNA sequences; *ii*) AuNPs as a core/seed that can be tailored with a wide variety of surface functionalities to provide highly selective nanoprobes to be used in combination with various signal transducers (QCM, SPR, etc...); *iii*) AuNPs in electrochemical detection methods that benefit from signal enhancement generated by metal deposition on the nanoparticle surface (silver enhancement); *iv*) AuNPs with alternative detection protocols (e.g. lateral flow strip).

## **Visual signal readout and scanometric detection**

A high sensitivity in the detection of nucleic acid target molecules can be achieved by using a simple visual signal readout. Colorimetric assays are based on the color change induced by the bio-recognition event obtained when complementary strands hybridize. A variety of colorimetric assays relying on AuNP signal amplification have been described,<sup>63,64</sup> but in many cases PCR amplification is required.<sup>65</sup>

Colorimetric methods offer the possibility to detect DNA molecules with naked eye visualization, thus allowing the development of convenient detection approaches requiring only the mixing of several solutions. However, the semi-quantitative detection allowed by visual inspection is not appropriate for applications requiring signal quantification. It is for this reason that colorimetric assays are coupled with quantifying detection systems. In particular, the scanometric detection method uses a convenient flatbed scanner for signal quantification.<sup>66</sup>

Simple colorimetric hybridization assays which exploit the color change caused by nanoparticle aggregation can be designed and thiol-linked ODN –modified AuNPs represent inexpensive and easy to synthesize nanoparticles to be used for the colorimetric detection of DNA targets.<sup>61</sup>

In 1996<sup>28</sup> it was shown that the distance-dependant optical properties of ODN-functionalized AuNPs can be used in colorimetric DNA assays. Single stranded target (linker) sequences are sandwiched between AuNPs of 13 nm in diameter conjugated to thiolated probe ODN via Au-S chemistry. Upon the addition of target DNA that cross-linked the probe ODN-modified AuNPs through sequence-specific hybridization, a color shift from red to purple was observed.<sup>67</sup> The denaturation of the formed DNA duplex obtained by heating above the melting temperature ( $T_m$ ) caused the dissociation of the AuNP aggregates and the color of the solution shifted back to red. The rate and the extent of the color change depend on the length of the linker sequence, with longer sequences inducing smaller shifts in the extinction spectrum that take longer to appear. Further studies indicated that the melting profiles of the ODN-modified AuNPs aggregates were

extraordinarily sharp, occurring over a temperature range much narrower than the transition for unlabeled or conventional fluorophore-labeled DNA.<sup>66</sup>

The functionalized AuNPs interparticle aggregation caused by probe-target hybridization can occur through cross-linking and non-cross-linking events.

Cross-link aggregation among AuNPs (**Fig. 2**) is driven by specific hybridization events between complementary strands and can be obtained by using a sandwich hybridization strategy<sup>67</sup> useful to detect target DNA that contains sequences complementary to two different AuNP-attached probes or a hybridization strategy based on the use of two sets of ODN-AuNPs systems carrying complementary ODN sequences.<sup>68</sup>

Non-cross-linking aggregation exploit changes in the AuNPs surface charge density that occurs upon DNA target interaction.<sup>69</sup> Many colorimetric methods are based on different propensities of single- and double-stranded DNA to adsorb on AuNPs, owing to different electrostatic properties.<sup>25,70</sup> The stability of AuNPs in solution depends on the balance of repelling and attracting forces that exist between particles as they approach one another. It is known that AuNPs are typically stabilized by adsorbed negatively-charged ions (e.g., citrate), which introduce a surface charge, thus preventing nanoparticle aggregation. ssDNA is sufficiently flexible to partially uncoil and expose its bases which can interact with gold through van der Waals interactions, while the negative charge on the backbone is sufficiently distant. This behavior is responsible for ssDNA capability to adsorb onto citrate prepared AuNPs, stabilizing them from aggregation at salt concentrations that would ordinarily screen the repulsive interactions of the citrate ions. On the contrary, the stable double-helix structure of dsDNA does not permit the uncoiling needed to expose the bases, thus electrostatic repulsion between a negatively charged phosphate backbone and adsorbed citrate ions prevails.

Non-cross-linking methods involve using only one type of DNA-AuNPs.<sup>71</sup> The target hybridization to the perfectly complementary AuNPs immobilized probe alters the nanoparticles' behavior against the salt-induced aggregation driven by London-van der Waals attracting forces. Any factor affecting

the surface properties of AuNPs such as nanoparticle size, species and concentration of ligands, pH, ionic strength, solvent composition, and temperature have been suggested as important in determining the aggregation of AuNPs.<sup>72</sup> Moreover, the preparation of DNA-nanoparticle conjugates with well-controlled DNA surface coverage and stability is critical for the positive outcome of the experiment.

A slightly different approach involves using conjugated polyelectrolyte to efficiently sequester single-stranded DNA (but not double-stranded or otherwise “folded” DNA) from nanoparticles, leaving it unable to stabilize the nanoparticles against aggregation.<sup>73</sup> The sensing strategy relies on the observations that both single-stranded DNA and double-stranded DNA prevent AuNP aggregation at low salt concentrations. In the absence of a target, single-stranded DNA molecules do not stabilize gold nanoparticles against aggregation in the presence of the polymer. In the presence of the complementary target sequence, however, a significant amount of double-stranded DNA is formed, which only weakly binds the conjugated polyelectrolytes and thus remains largely free to prevent the aggregation of gold-nanoparticles. This colorimetric assay is sensitive enough to allow the visual detection of low pM concentrations of target DNA.

AuNPs-based visual readout detection of DNA is also possible by exploiting biomineralization processes.<sup>74</sup> The method is based on the immobilization of a captured oligonucleotide on a solid surface followed by the hybridization with the target oligonucleotide. A cascade signal amplification process is enabled by the use of two differently modified AuNP probes, one of which is functionalized with biomineralization-capable silicatein. Target DNA identification is achieved through the visual readout of the signal generated by silver selective deposition on AuNP probes. Color changes resulting from catalytic silica synthesis came from a variation in the position of the surface plasmon resonance band caused by changes in the dielectric constant and surface loading density of AuNPs. The visual signal readout system was able to detect target oligonucleotides at a concentration as low as 50 aM (~180 molecules in 6  $\mu$ L) thus increasing the sensitivity of colorimetric sensing even when single-base mismatches would have been investigated.<sup>75,76</sup>

Typical colorimetric DNA detection methods are based on a three-component sandwich assay format that includes a target DNA and two sets of ODN-AuNPs probes. The target DNA also serves as a linker strand that triggers particle aggregation and a concomitant color change. Thus, the colorimetric detection limit is directly associated with the minimum number of the linkers required to initiate particle aggregation, which can be observed with the naked eye. At low linker concentrations (about 10 nM) aggregation of 14 nm nanoparticles does not exhibit sharp colorimetric melting transitions. Sensitivity can be increased by using a nicking endonuclease-assisted nanoparticle amplification (NEANA) procedure.<sup>77</sup> NEANA has been shown to be capable of recognizing long single-stranded oligonucleotides with single-base mismatch selectivity with a detection limit of 0.5 fmol.

The detection system requires two sets of ODN-modified AuNP probes and an additional oligonucleotide strand which acts as a linker. The nicking endonuclease recognizes a specific nucleotide sequence in double-stranded (ds) DNA and is specifically designed to cleave only the linker strand. The fragments produced after nicking spontaneously dissociate from the target DNA at an elevated temperature, enabling another linker strand to hybridize to the target in a strand-scission cycle. Upon completion of the strand-scission cycle, two sets of different ODN-modified AuNPs with sequences complementary to that of the linker strand are added to the solution to detect the presence of a target DNA. If the linker is non-complementary to the target DNA, particle aggregation will occur. A single-base mismatch is enough to inhibit the cleavage of the linker strand, leading to particle aggregation upon addition of oligonucleotide-modified gold nanoparticles with sequences complementary to that of the linker strand.

The easy visual inspection of the presence of oligonucleotide functionalized gold nanoparticles has also allowed the fabrication of disposable nucleic acid biosensors, combining the optical properties of the nanoparticles with the chromatographic separation allowed by the lateral flow strip.<sup>78</sup> AuNPs modified with a hairpin oligonucleotide carrying a biotin group at 3'-end were allowed to interact with perfectly-matched DNA and single-base-mismatched DNA to generate different quantities of

“active” biotin groups.<sup>51</sup> The activated biotins were captured on the test zone of a lateral flow strip via the specific binding with pre-immobilized streptavidin. The optical properties of the AuNPs are useful for an easy visual inspection of the color difference existing between the test line and the control line after the target capture, and a discrimination of as low as 10 pM between perfectly-matched DNA and single-base-mismatched DNA is obtained.<sup>79</sup>

A similar detection limit (10 pM) has been reached by exploiting the electrostatic interactions between positively charged AuNPs and negatively charged DNA bound to neutral PNA capture probes.<sup>80</sup>

The combined use of two-component ODN-modified AuNPs and single-component ODN-modified magnetic microparticles (MMPs) has offered the possibility to develop a zeptomolar sensitive biobarcode-based DNA detection method.<sup>81</sup> The two ODNs, one complementary to the target sequence and the other complementary to a bar-code sequence, were immobilized on AuNP surfaces. MMPs were instead functionalized with ODN that were complementary to one portion of the target sequence and different from the region recognized by the AuNP. After the sandwich reaction between the target sequence AuNP and MMP, the reacted and unreacted MMPs were separated by a magnetic field and the unreacted solution components washed away. Then the bar-code DNA was released by heating at 55°C and all of the MMPs were removed from the solution. Finally, the bar-code DNA sequence was analyzed with a chip-based visual scanometric method that relies on ODN-modified AuNP probes and silver enhancement. The great advantage of the bio-bar code assay is that it allows PCR-like sensitivity without a need for enzymatic amplification, thus avoiding the drawbacks of a PCR reaction.

Ultrasensitivity is a fundamental requirement when direct detection of non-amplified genomic DNA will be carried out. A similar sensitivity has been achieved by using an AuNP scatter-based detection method that allows an allele-specific hybridization methodology for multiplex SNP profiling in total human genomic DNA without the need for target amplification.<sup>60</sup> The SNP genotyping strategy relies on the sequential hybridizations of two sequence-specific probes, allele-

specific surface-immobilized capture probes and gene-specific oligonucleotide functionalized gold nanoparticle probes, which selectively ‘sandwich’ the target. The importance of a double hybridization step is related to the complexity of human genomic DNA. In fact, due to the presence of non-target sequences in the sample it is likely that those sequences bind both to capture probes as well as to a specific target during the first hybridization step. The second hybridization step provides the discrimination power required to distinguish between targets and non-target sequences and allows SNP identification. A silver enhancement step enhances the AuNPs ability to scatter light by several orders of magnitude and allows a 50 fM (500 ng in 5 ml) detection limit to be obtained.<sup>58</sup>

### **Chemiluminescence detection**

The detection of chemiluminescence (CL) and electrogenerated chemiluminescence (ECL) signals offers other opportunities for the AuNPs-based ultrasensitive detection of nucleic acids.

The dissolution of  $\text{Cu}^{2+}$  ions from CuS nanoparticles can be used to generate a CL signal by coupling the complex-formation reaction of cupric ions and cyanide with the chemiluminescence reaction of luminal and  $\text{Cu}(\text{CN})_4^{2-}$ .<sup>82</sup> The process benefit from the decoration of mercaptoacetic acid functionalized AuNPs with CuS nanoparticles bearing aminoethanethiol moieties on their surface. The amidization reaction allows the loading of 77 CuS nanoparticles on the AuNPs’ surface.<sup>83</sup> The use of the combined CuS-AuNPs system and the detection of the CL signal obtained after a preconcentration process of  $\text{Cu}^{2+}$  ions has been used to develop a DNA detection method based on the hybridization between DNA probes, self-assembled on a Au electrode and a mixture of completely complementary and single-base mismatched DNA molecules. The successive coupling of mutant sites in duplex DNA to nucleotide modified Au NPs-CuS NPs assemblies has allowed the detection of SNPs with a detection limit of 19 aM.<sup>83</sup>

DNA detection can also be based on the electrogenerated chemiluminescence (ECL) signal detection. ECL involves the electrochemical generation of excited states and differs from CL



because in ECL, the event that triggers the production of active species is the switching of an electrode voltage.<sup>84</sup> In many ECL applications, a co-reactant is employed which, upon oxidation or reduction, produces an intermediate species that can react with an ECL luminophore resulting in the generation of excited states. The combined use of CdS:Mn nanocrystals (NCs) acting as ECL luminophores,  $S_2O_8^{2-}$  ions acting as co-reactant and AuNPs acting both as ECL quenchers and enhancers (**Fig. 3**) has offered the possibility to develop a 50 aM sensitive DNA platform.<sup>85</sup>

AuNPs synthesized via reduction of  $H AuCl_4$  by luminol exhibit ECL activity and can be coupled with ssDNA without the loss of ECL activity or change in the specificity of the hybridization reaction. A sandwich DNA detection protocol can be thus obtained by using biotinylated DNA capture probes immobilized on streptavidin coated AuNPs. The sandwich target interaction with both the capture probe and the luminol-labeled DNA signal probe followed by ECL signal generation provides a 0.19 fM sensitive DNA detection assay.<sup>86</sup> The robustness of the method has been shown by the detection of target DNA from human blood serum samples. ECL applications in the detection of genetically modified organisms (GMOs) have been also demonstrated.<sup>87</sup>

### **Electrochemical detection**

Electrocatalytic labels can significantly change the electrocatalytic activity of sensing electrodes during a detection process. However, the label electrocatalytic activity may be significantly reduced by the conjugation with biomolecules and a reduced electron tunneling between the electrode and the electrocatalytic label may arise as a consequence of the electrode-label distance. In this context, sandwich-type DNA sensors have been developed employing AuNPs as electrocatalytic labels.<sup>12</sup>

A detection protocol was obtained by sandwiching target DNA between biotinylated capture probes which had been previously immobilized onto a streptavidin modified indium-tin oxide (ITO) electrode and probe-conjugated AuNPs.<sup>88</sup> Hydrazine electro-oxidation readily occurs on bare AuNPs, whereas it does not on DNA-conjugated AuNPs. Thus, when DNA-conjugated AuNPs were used as electrocatalytic labels, the anodic current of hydrazine was not easily observed

because of the high overpotential caused by the slow electron-transfer kinetics on DNA-conjugated AuNPs as well as the slow electron tunneling between the AuNP and the indium-tin oxide (ITO) electrode. The method allows single-base mismatched DNA and non-complementary DNA to be distinguished from complementary target DNA with a 1 fM sensitivity. The combined use of AuNP labelling and magnetic beads (Mbs) offers a versatile tool for electrochemical DNA biosensing. Similar possibilities can be obtained by using a capture-probe-conjugated Mbs as the target-binding surface and ferrocene (Fc)-modified ITO electrodes as the signal-generating surface. The sandwich target DNA detection is followed by the transfer of the resulting magnetic assembly to the electrode surface where *p*-aminophenol is generated and electro-oxidized. Even in this case a 1 fM sensitivity has been reported for DNA detection.<sup>89</sup>

A 450 aM DNA sensitivity has been obtained by using a conductive polymer with an immobilized dendrimer/AuNP assembly and hydrazine label units. The hydrazine label was used as an electrocatalyst and was immobilized on the sensing layer through avidin-biotin affinity interaction.<sup>90</sup> The highly branched nature of dendrimer allowed the immobilization of a large number of AuNPs onto the electrode surface thus contributing to the generation of ultrasensitive DNA detection.

The anodic stripping detection offers another opportunity to develop ultrasensitive DNA detection methods.<sup>91</sup> A detection strategy based on the interaction of ODN-modified AuNPs detection probes with target DNA previously adsorbed on polystyrene microwells was used to analyse the anodic stripping voltammetry of Au<sup>3+</sup> ions released from AuNPs after an oxidative treatment. The measured signal in the electrochemical method is proportional to the size of AuNPs. For this reason a gold-based autometallographic enlargement of anchored AuNPs increases the method sensitivity by allowing a 600 aM detection limit (~1.4 zmol or 840 DNA sequences per microwell) to be obtained.

Nanoporous gold (NPG) electrodes have been shown to further increase sensitivity in DNA detection.<sup>92</sup> Single-stranded DNA capture probes were immobilized on the NPG electrode surface

and then hybridized with target DNA (**Fig. 4**). Subsequently, AuNPs modified with two bio-bar code DNAs, one of which was complementary to the target DNA, were allowed to interact with the target DNA through a sandwich hybridization strategy. Upon the electrostatic interaction of  $[\text{Ru}(\text{NH}_3)_6]^{3+}$  with the reporter DNA, an electrochemical signal was measured. The great advantage of the method relies on the fact that each AuNP was loaded with  $\sim 100$  reporter DNA strands, offering a significant amplification for DNA detection and allowing a 28 aM detection limit to be reached.

### **Quartz crystal microbalance-based methods**

AuNPs have been also used as a “seeding catalyst” in order to enhance piezoelectric transducer frequency shifts. Microgravimetric quartz crystal microbalance (QCM) can provide fM sensitivity in DNA detection when avidin labeled AuNPs bind the target containing biotinylated double-stranded assembly, which was immobilized on the piezoelectric crystal surface.<sup>93</sup> The associated AuNPs act as a ‘seeding catalyst’ for a secondarily-catalyzed deposition of gold that increases the dimension of the gold particles thus producing an amplified frequency shifts (**Fig. 5**). A further increase in sensitivity requires the combined use of the nanoparticle modification of the QCM surface with DNA-capped AuNPs signal amplification.<sup>94,95</sup> The target DNA was sandwiched between AuNPs immobilized on the QCM sensor surface and ODN-functionalized AuNPs. The method resulted in a DNA sensitivity of  $10^{-16}$  M.

A novel scheme for signal amplification using random tetramer-modified AuNPs, called “nanoamplicons” has been proposed for PCR-free DNA detection.<sup>96</sup> The method is based on the microgravimetric detection of the adsorption of a probe-target-nanoamplicons complex on a QCM gold electrode. Signal amplification is accomplished by the integration of a large number of amplicons onto one target, enabling the achievement of a sensitivity of 0.17 aM. In addition to an extremely high sensitivity, a great advantage of this approach is the possibility to design

nanoamplicons that could be universally adapted to any target sequence, allowing the generalization of the bioassays and the applicability to all diagnostic tests.

### **Surface plasmon resonance detection**

Surface plasmon resonance (SPR) is an optical technique used to monitor interactions established between receptors immobilized on a metal surface and analytes which are put in contact with the sensor surface.<sup>97</sup> SPR imaging (SPRI)<sup>98</sup> combines the advantages offered by the traditional SPR in detecting molecular and biomolecular interactions<sup>99, 100, 101, 102</sup> with those associated to an imaging system, including the coupling with microfluidic devices<sup>103</sup> and the simultaneous monitoring of the interaction of biomolecules arrayed onto the metal surface.<sup>104</sup> However, the use of SPRI for genomic assays is limited by the reduced sensitivity in detecting hybridized DNA or RNA samples. Thus, several label-free and PCR-free approaches, aimed at amplifying the SPRI response to DNA and RNA hybridization with high-throughput, low sample consumption, and ultrasensitivity based on the use of AuNPs have been developed.<sup>105</sup> D'Agata et al.<sup>39</sup> showed the ultrasensitive capabilities offered by a method combining surface-immobilized PNA probes with continuous-flow microfluidics and nanoparticle-enhanced SPRI biosensing in detecting ODNs. DNA detection methods greatly benefit from the use of microfluidic technologies because they allow the analysis of a very small amount of DNA molecules. The detection of target or control DNAs was obtained by adopting a sandwich hybridization strategy using AuNPs conjugated to an oligonucleotide complementary to the final tract of the DNA target not involved in the hybridization with the SPRI sensor surface-immobilized PNA probe (**Fig. 6**). The sandwich hybridization strategy allowed the discrimination between fully-matched and single-base mismatched sequences even at the 1 fM concentration. In addition, the microfluidic management of the fluids allowed a multiplexed determination of the SPRI responses. The discrimination was obtained by using 150 zeptomoles of the DNA target.

The same approach revealed its feasibility in the detection of non-amplified genomic DNA samples carrying different amounts of genetically modified (GM) sequences (Roundup Ready soybean, RR).<sup>40</sup> The system was able to selectively identify the GM target sequence down to a zM concentration in solutions containing GM and GM-free genomic DNA with an aM concentration, even in the presence of a large excess of non-complementary DNA. Taking into account that solutions containing the non-amplified GM DNA sequence at the 41zM concentration can be selectively detected by using only 11 molecules of the genomic GM DNA, it is easy to conclude that the combined use of nanoparticle-enhanced SPRI and PNA probes provides a new tool for the rapid, specific and ultra-sensitive detection of genomic DNA. This results in a direct method for the detection of the GMO content, which parallels the specificity of PCR-based methods.

A novel ultrasensitive surface plasmon biosensor, termed “nanoparticle-enhanced diffraction grating” (NEDG), for the detection of DNA was developed by Wark et al.<sup>106</sup> by combining the optical properties of planar surface plasmon polaritons generated on gold gratings with the optical properties of gold nanoparticles. The approach is based on the adsorption of DNA-modified gold nanoparticles in a sandwich strategy onto functionalized gold diffraction gratings, as well as on the analysis of the nanoparticle-enhanced diffraction signal generated in a Kretschmann configuration for surface plasmon resonance. An extended study has been performed to demonstrate the high sensitivity of the NEDG biosensor. A series of femtomolar solutions of a target ssDNA molecule were employed, showing that nonspecific adsorption of DNA-modified nanoparticles was not observed even when control experiments including mismatched DNA sequences were performed. The system was able to detect unmodified DNA at a concentration of 10 fM.

## **Conclusions**

The aim of this review is to give an overview of the current use of AuNPs for applications in the field of DNA sensing, due to the important role of DNA analysis as a promising tool in several areas like medical and forensic diagnostics, environmental control and food safety.

Literature-cited examples exploit the properties of AuNPs, offering excellent advantages to conventional strategies based on PCR-amplification and fluorophore labelling. Although, the signal enhancement power of AuNPs allows the achievement of high sensitivity in the detection of specific DNA sequences down to the zeptomolar range, only a few examples have been applied to the real sample. In this scenario, in order to think about future trends of AuNPs in diagnostic applications, significant improvements still need to be made. These include control over parameters such as NPs size and their dispersion in the synthesis process together with functionalization.

Besides sensitivity and selectivity, the multiplexing capacity is another important aspect that the detection systems should be able to exhibit, detecting multiple DNA analytes simultaneously.

## Acknowledgments

We acknowledge support from MIUR (FIRB RBRN07BMCT and RBPR05JH2P ITALNANONET).

## References

---

<sup>1</sup> Faraday M (1857) *Philos. Trans. Royal Soc. London*, 147:145–181.

<sup>2</sup> Mie G (1908) *Ann Phys* 25:377–445.

<sup>3</sup> Ghosh SK, Pal T (2007) *Chem Rev* 107: 4797-4862.

<sup>4</sup> Rosi NL, Mirkin CA (2005) *Chem Rev* 105:1547–1562.

<sup>5</sup> Mrinmoy D, Ghosh PS, Rotello VM (2008) *Adv Mater* 20:4225–4241.

<sup>6</sup> Baptista P, Pereira E, Eaton P, Doria G, Miranda A, Gomes I, Quaresma, P, Franco R (2008) *Anal Bioanal Chem* 391:943–950.

<sup>7</sup> Niemeyer CM. (2001) *Angew Chem Int Ed* 40:4128–4185.

<sup>8</sup> Zhang DY, Seelig G (2011) *Nat Chem* 3, 103-113.

- 
- <sup>9</sup> Krishnan Y, Simmel FC (2011) *Angew Chem Int Ed* 50:3124-3156.
- <sup>10</sup> Metzker ML (2010) *Nature Rev. Genet.* 11, 31-46.
- <sup>11</sup> Shi L, Perkins RG, Fang H, Tong W, (2008) *Curr Opin Biotechnol* 19:10–18.
- <sup>12</sup> Merkoçi, A (2010) *Biosens Bioelectron* 26:1164-1177.
- <sup>13</sup> Pérez-López B, Merkoçi, A (2011) *Anal Bioanal Chem* 399:1577–1590.
- <sup>14</sup> Zhao W; Brook MA; Li YF (2008) *ChemBioChem* 9: 2363-2371.
- <sup>15</sup> Sassolas A, Leca-Bouvier BD, Blum LJ(2008) *Chem Rev* 108:109-139.
- <sup>16</sup> Cosnier S, Mailley P (2008) *Analyst* 133:984-991.
- <sup>17</sup> Song SP, Qin Y, He Y, Huang Q, Fan CH, Chen HY (2010) *Chem Soc Rev* 39:4234-4243.
- <sup>18</sup> Teles FRR, Fonseca LR (2008) *Talanta* 77:606-623.
- <sup>19</sup> Wang Z, Ma L (2009) *Coord Chem Rev* 253: 1607-1618.
- <sup>20</sup> Daniel MC, Astruc D (2004) *Chem Rev* 104:293–346.
- <sup>21</sup> Marek Grzeleczak, Jorge Pérez-Juste, Paul Mulvaney, Luis M. Liz-Marzán (2008) *Chem Soc Rev* 37:1783-1791.
- <sup>22</sup> Turkevich J, Stevenson PC, Hillier J (1951) *Discuss Faraday Soc* 11:55–75.
- <sup>23</sup> Frens G (1973) *Nature* 241:20-22.
- <sup>24</sup> Wilson R (2008) *Chem Soc Rev* 37:2028–2045.
- <sup>25</sup> Li H, Rothberg L (2004) *Proc Natl Acad Sci USA* 101:14036-14039.
- <sup>26</sup> Yang-Wei L, Chi-Wei L, Huan-Tsung C, (2009) *Anal Methods* 1:14–24.
- <sup>27</sup> Cioffi N, Colaianni L, Ieva E, Pilolli R, Ditaranto N, Angione MD, Cotrone S, Buchholt K, Spetz AL, Sabbatini L, Torsi L (2011) *Electrochim Acta* 56: 3713-3720.
- <sup>28</sup> Mirkin CA, Letsinger RL, Mucic RC, Storhoff JJ (1996) *Nature* 382:607–609.
- <sup>29</sup> Reynolds RA, Mirkin CA, Letsinger RL (2000) *J Am Chem Soc* 122:3795–3796.
- <sup>30</sup> Jin R, Wu G, Li Z, Mirkin CA., Schatz GC, (2003) *J Am Chem Soc* 125:1643–1654.

- 
- <sup>31</sup> Storhoff JJ, Elghanian R, Mucic RC, Mirkin CA, Letsinger RL (1998) *J Am Chem Soc* 120: 1959–1964.
- <sup>32</sup> Pellegrino T, Kudera S, Liedl T, Javier AM, Manna L, Parak WJ (2005) *Small* 1:48-63.
- <sup>33</sup> Peña SRN, Raina S, Goodrich GP, Fedoroff NV, Keating CD (2002) *J Am Chem Soc* 124:7314–7323.
- <sup>34</sup> Hurst SJ, Lytton-Jean AKR, Mirkin CA (2006) *Anal Chem* 78:8313–8318.
- <sup>35</sup> Demers LM, Mirkin CA, Mucic RC, Reynolds RA, Letsinger RL, Enghanian R, Viswanadham G (2000) *Anal Chem* 72:5535–5541.
- <sup>36</sup> Jin R, Wu G, Li Z, Mirkin CA, Schatz GC (2003) *J Am Chem Soc* 125:1643-1654.
- <sup>37</sup> Sperling RA, Gil PR, Zhang F, Zanella M, Parak WJ (2008) *Chem Soc Rev* 37:1896–1908.
- <sup>38</sup> Alivisatos AP, Johnsson KP, Peng X, Wilson TE, Loweth CJ, Bruchez MP, Schultz PG (1996) *Nature* 382:609–611.
- <sup>39</sup> D’Agata R, Corradini R, Grasso G, Marchelli R, Spoto G (2008) *ChemBioChem* 9:2067–2070.
- <sup>40</sup> D’Agata R, Corradini R, Ferretti C, Zanolli L, Gatti M, Marchelli R, Spoto G (2010) *Biosens Bioelectron* 25:2095–2100.
- <sup>41</sup> Nielsen PE (1999) *Acc Chem Res* 32:624–630.
- <sup>42</sup> Zanolli L, D’Agata R, Spoto G (2008) *Minerva Biotecnol* 20:165–174.
- <sup>43</sup> Chakrabarti R, Klibanov AM (2003) *J Am Chem Soc* 125:12531–12540.
- <sup>44</sup> Ganesh KN, Nielsen PE (2000) *Curr Org Chem* 4:941–943.
- <sup>45</sup> Sforza S, Corradini R, Tedeschi T, Marchelli R (2001) *Chem Soc Rev* 40:221-232.
- <sup>46</sup> Kanjanawarut R, Su X (2009) *Anal Chem* 81:6122–6129.
- <sup>47</sup> Su X, Kanjanawarut R (2009) *ACS Nano* 3:2751–2759.
- <sup>48</sup> Tyagi S, Kramer FR (1996) *Nat Biotechnol*, 14:303–308.
- <sup>49</sup> Dubertret B, Calame M, Libchaber AJ (2001) *Nat Biotechnol* 19:365–370.
- <sup>50</sup> Maxwell DJ, Taylor JR, Nie S, (2002) *J Am Chem Soc* 124:9606–9612.



- 
- <sup>51</sup> He Y, Zeng K, Gurung AS, Baloda M, Xu H, Zhang X, Liu G (2010) *Anal Chem* 82:7169–7177.
- <sup>52</sup> Breaker RR (1997) *Nat Biotechnol* 15:427–431.
- <sup>53</sup> Niazov T, Pavlov V, Xiao Y, Gill R, Willner I (2004) *Nano Lett* 4:1683–1687.
- <sup>54</sup> Thaxton CS, Mirkin CA (2005) *Nat Biotechnol* 23:681–682.
- <sup>55</sup> Stierhof YD, Humbel BM, Schwarz HJ (1991) *J Electron Microscop Technol* 17:336–343.
- <sup>56</sup> Yguerabide J, Yguerabide EE (1998) *Anal Biochem* 262:157–176.
- <sup>57</sup> Taton TA, Lu G, Mirkin CA (2001) *J Am Chem Soc* 123:5164–5165.
- <sup>58</sup> Storhoff JJ, Marla SS, Bao P, Hagenow S, Mehta H, Lucas A, Garimella V, Patno T, Buckingham W, Cork W, Muller UR (2004) *Biosens Bioelectron* 19:875–883.
- <sup>59</sup> Huber M, Wei TF, Muller UR, Lefebvre PA, Marla SS, Bao YP (2004) *Nucleic Acids Res* 32:e137.
- <sup>60</sup> Bao YP, Huber M, Wei TF, Marla SS, Storhoff JJ, Muller UR (2005) *Nucleic Acids Res* 33, e15.
- <sup>61</sup> Storhoff JJ, Lucas AD, Garimella V, Bao YP, Muller UR (2004) *Nat Biotechnol* 22: 883–887.
- <sup>62</sup> Fang Z, Soleymani L, Pampalakis G, Yoshimoto M, Squire JA, Sargent EH, Kelley SO (2009) *ACS Nano* 3:3207–3213.
- <sup>63</sup> Zhu X, Liu Y, Yang J, Liang Z, Li G (2010) *Biosens Bioelectron* 25: 2135–2139.
- <sup>64</sup> Reynolds RA, Mirkin CA, Letsinger RL (2000) *Pure Appl Chem* 72: 229–235.
- <sup>65</sup> Li J, Chu X, Liu Y, Jiang JH, He Z, Zhang Z, Shen G, Yu RQ (2005) *Nucleic Acids Res* 33:e168.
- <sup>66</sup> Taton TA, Mirkin CA, Letsinger RL (2000) *Science*, 289:1757–1760.
- <sup>67</sup> Elghanian R, Storhoff JJ, Mucic RC, Letsinger RL, Mirkin CA (1997) *Science* 111:1078–1081.
- <sup>68</sup> Lee J, Lytton-Jean AKR, Hurst SJ, Mirkin CA (2007) *Nano Lett* 7: 2112–2115.
- <sup>69</sup> Sato K, Hosokawa K, Maeda M (2005) *Nucleic Acids Res* 33:e4.
- <sup>70</sup> Li H, Rothberg LJ (2004) *J Am Chem Soc* 126: 10958–10961.
- <sup>71</sup> Sato K, Hosokawa K, Maeda M. (2003) *J Am Chem Soc* 125:8102–8103.
- <sup>72</sup> Ghosh SK, Pal T, (2007) *Chem Rev* 107:4797–4862.

- 
- <sup>73</sup> Xia F, Zuo X, Yang R, Xiao Y, Kang D, Vallee-Belisle A, Gong X, Yuen JD, Hsu BBY, Heeger AJ, Plaxco KW (2010) *Proc Natl Acad Sci USA* 107:10837–10841.
- <sup>74</sup> Zhou X, Xia S, Lu Z, Tian Y, Yan Y, Zhu J (2010) *J Am Chem Soc* 132:6932–6934
- <sup>75</sup> Baecissa A, Dave N, Smith BD, Liu J (2010) *ACS Appl Mater Interfaces* 2:3594–3600.
- <sup>76</sup> Sliem MA, Ebeid EM, Harith M (2007) *J Biomed Nanotech* 3:360–366.
- <sup>77</sup> Xu W, Xue X, Li T, Zeng H, Liu X (2009) *Angew Chem Int Ed* 48: 6849 –6852
- <sup>78</sup> Mao X, Ma Y, Zhang A, Zhang L, Zeng L, Liu G (2009) *Anal Chem* 81:1660–1668.
- <sup>79</sup> Mao X, Xu H, Zeng Q, Zeng L, Liu G (2009) *Chem Commun* 21:3065–3067.
- <sup>80</sup> Kim SK, Cho H, Jeong J, Kwon JN, Jung Y, Chung BH (2010) *Chem Commun* 46:3315–3317.
- <sup>81</sup> Nam JM, Stoeva SI, Mirkin CA (2004) *J Am Chem Soc* 126:5932–5933.
- <sup>82</sup> Ding C F, Zhong H, Zhang SS (2008) *Biosens Bioelectron* 23:1314–1318.
- <sup>83</sup> Ding C, Wang Z, Zhong H, Zhang S (2010) *Biosens Bioelectron* 25:1082–1087.
- <sup>84</sup> Richter MM (2004) *Chem Rev* 104:3003–3036.
- <sup>85</sup> Shan Y, Xu JJ, Chen HY (2009) *Chem Commun* 905–907.
- <sup>86</sup> Chai Y, Tian D, Wang W, Cui H (2010) *Chem Commun* 46:7560–7562.
- <sup>87</sup> Zhu D, Tang Y, Xing D, Chen WR (2008) *Anal Chem* 80:3566–3571.
- <sup>88</sup> Das J, Yang H (2009) *J Phys Chem C* 113:6093–6099.
- <sup>89</sup> Selvaraju T, Das J, Jo K, Kwon K, Huh CH, Kim TK, Yang H (2008) *Langmuir* 24:9883–9888.
- <sup>90</sup> Shiddiky MJA, Aminur R Md, Shim Y (2007) *Anal Chem* 79:6886–6890.
- <sup>91</sup> Rochelet-Dequaire M, Limoges B, Brossier P (2006) *Analyst* 131:923–929.
- <sup>92</sup> Hu K, Lan D, Li X, Zhang S (2008) *Anal Chem* 80:9124–9130.
- <sup>93</sup> Weizmann Y, Patolsky F, Willner I (2001) *Analyst* 126:1502–1504.
- <sup>94</sup> Liu T, Tang J, Jiang L (2002) *Biochem Biophys Res Commun* 295:14–16.
- <sup>95</sup> Liu T, Tang J, Jiang L (2004) *Biochem Biophys Res Commun* 313:3–7.
- <sup>96</sup> Mo ZH, Wei XL (2006) *Anal Bioanal Chem* 386:2219–2223.

- 
- <sup>97</sup> Homola J (2006) *Surface Plasmon Resonance Based Sensors*, Springer, Berlin.
- <sup>98</sup> Scarano S, Mascini M, Turner APF, Minunni M (2009) *Biosens Bioelectron* 25:957-966.
- <sup>99</sup> Grasso G, Rizzarelli E, Spoto G (2008) *BBA Proteins Proteom* 1784:1122-1126
- <sup>100</sup> Ciaccio C, Tundo GR, Grasso G, Spoto G, Marasco D, Ruvo M, Gioia M, Rizzarelli E, Coletta M (2009) *J Mol Biol* 385: 1556-1567:
- <sup>101</sup> Grasso G, Bush AI, D'Agata R, Rizzarelli E, Spoto G (2009) *Eur Biophys J Biophys* 38:407-414.
- <sup>102</sup> Arena G, Contino A, Longo E, Sgarlata C, Spoto G, Zito V(2004) *Chem Commun* 16:1812-1813.
- <sup>103</sup> Grasso G, D'Agata R, Zanolli L, Spoto G (2009) *Microchem J* 93: 82-86.
- <sup>104</sup> D'Agata R, Grasso G, Iacono G, Spoto G, Vecchio G (2006) *Org Biomol Chem* 4:610–612.
- <sup>105</sup> Fang S, Lee HJ, Wark AW, Corn RM (2006) *J Am Chem Soc* 128:14044-14046.
- <sup>106</sup> Wark AW, Lee HJ, Qavi AJ, Corn RM (2007) *Anal Chem* 79:6697-6701.

## CAPTIONS

**Figure 1:** Schematic illustration of strategies used to functionalize AuNPs to be used for DNA detection.

**Figure 2:** The cross-link aggregation of oligonucleotide-functionalized AuNPs occurring in the presence of complementary target DNA results in a change of solution color from red to blue.

**Figure 3:** The electrochemiluminescence from CdS:Mn nanocrystals was quenched (b) when AuNPs labeled with hairpin-DNA probe were in close proximity to the nanocrystal film. Upon the occurrence of the hybridization with target DNA (c), a signal enhancement was obtained (glassy carbon electrode, GC). (Reprinted with permission from ref. 85)

**Figure 4:** Schematic representation of the chronocoulometry detection of DNA. The amplification of the detected signal was generated by  $[\text{Ru}(\text{NH}_3)_6]^{3+}$  bound to oligonucleotides adsorbed on AuNPs.

**Figure 5:** Schematic representation of the quartz-crystal-microbalance enhanced detection of DNA. The amplification resulted from the association of an AuNP-avidin conjugate and the catalytic deposition of gold.

**Figure 6:** Schematic representation of the procedure adopted for the nanoparticle-enhanced surface plasmon resonance imaging ultrasensitive detection of DNA.

**Table 1:** Working principles and performances of AuNPs-based ultrasensitive DNA detection methods.

**Figure 1**

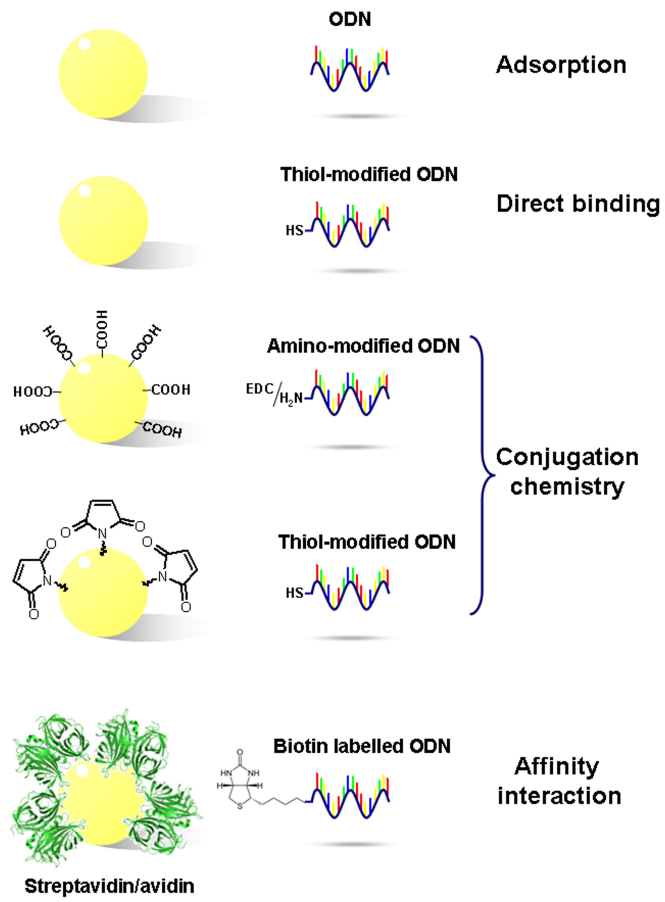


**Figure 2**

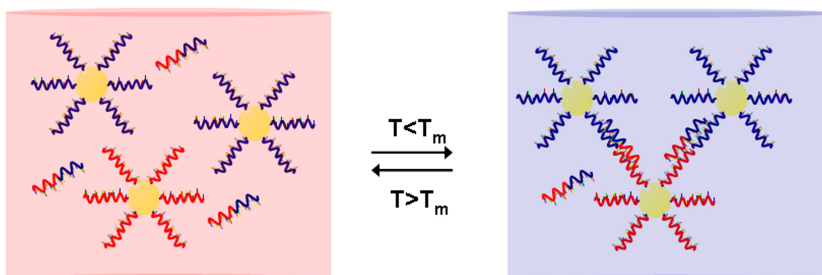


Figure 3

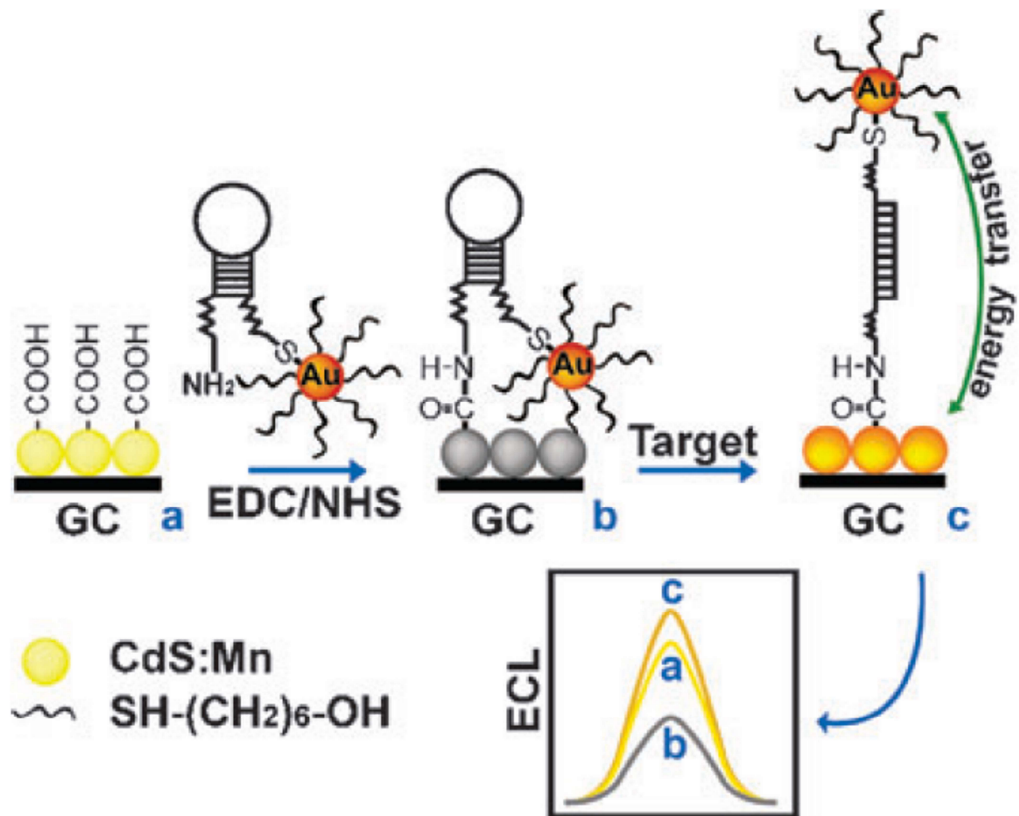


Figure 4

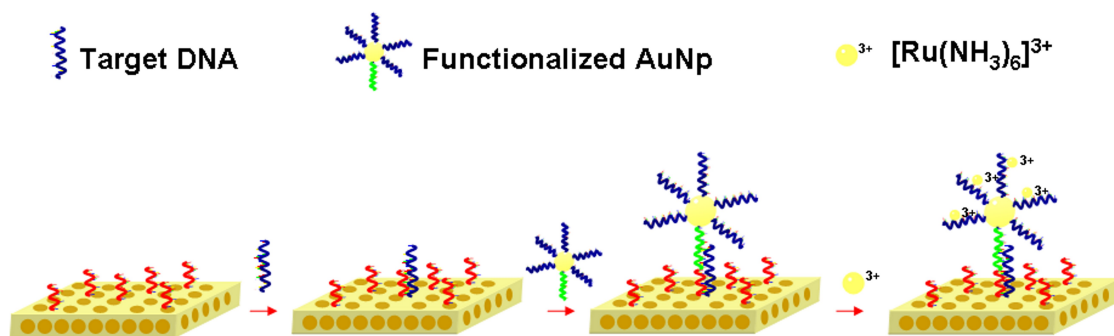




Figure 5

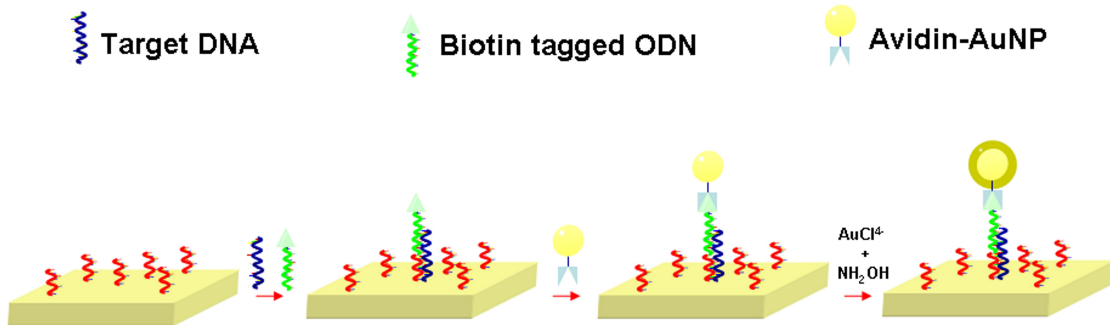
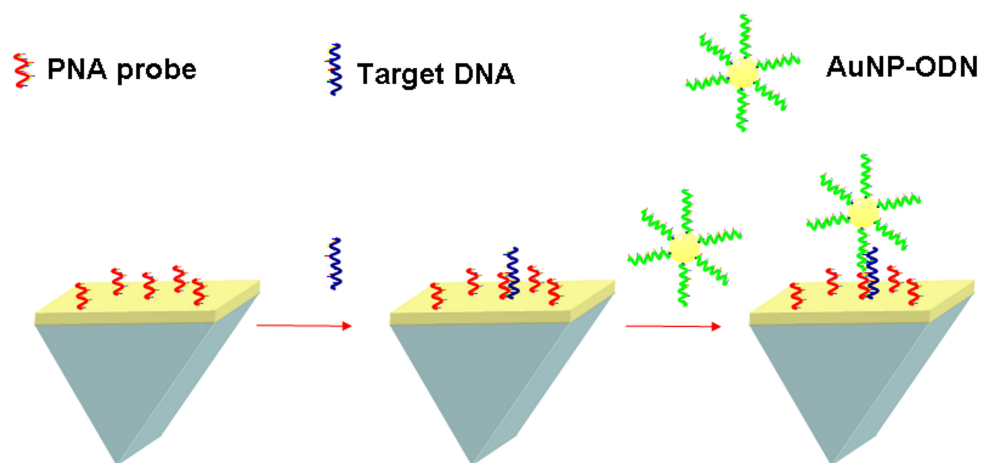


Figure 6



**Table 1**

Detection methods	Working principles	AuNP functionalization	Sensitivity	Analysis time	Ref.
<b>Visual readout</b>	Salt induced aggregation	Adsorption	<100 fmol	5 min.	25
	Interaction between conjugated polyelectrolyte and single-stranded DNA	Adsorption	pM	5-10 min.	73
	Biom mineralization-assisted amplification	Thiol-modified oligonucleotide	50 aM	-	74
	Nicking endonuclease-assisted nanoparticle amplification	Thiol-modified oligonucleotide	0.5 fmol	hours	77
	Lateral flow strip	Thiol-modified oligonucleotide	10 pM	15 min.	78
<b>Scanometric</b>	Electrostatic interactions between positively charged AuNPs and DNA bound to neutral PNA capture probes	Cetyltrimethylammonium bromide coating	10 pM	-	80
	Bio-bar code assay	Thiol-modified oligonucleotide	500 zM	3-4 h	81
	Hybridizations between surface-immobilized probes and AuNPs- probes	Thiol-modified oligonucleotide	50 fM	-	60
<b>Chemiluminescence</b>	Oxidative release of Cu <sup>2+</sup>	Thiol-modified oligonucleotide/CuS NPs labels	19 aM	~15 h	83
<b>Electrogenerated chemiluminescence</b>	Förster energy transfer of ECL excited surface plasmon resonances in AuNPs to CdS:Mn NCs	Thiol-modified oligonucleotide	50 aM	hours	85
	Sandwich hybridization / Luminol ECL activity	Affinity interaction	0.19 fM	hours	86
	Selective capturing by magnetic beads	Thiol-modified oligonucleotide	1 fmol	3-4 h	87
<b>Electrochemical</b>	Hydrazine electrooxidation	Thiol-modified oligonucleotide	1 fM	~ 4 h	88
	Generation and electrooxidation of p-aminophenol	Thiol-modified oligonucleotide	1 fM	-	89
	Electrocatalytic reduction of hydrogen peroxide	Thiol-modified oligonucleotide	450 aM	hours	90
	Anodic stripping detection of chemically oxidized gold	Thiol-modified oligonucleotide	600 aM	~1-2 h	91
	Chronocoulometry of [Ru(NH <sub>3</sub> ) <sub>6</sub> ] <sup>3+</sup>	Thiol-modified oligonucleotide	28 aM	~ 4 h	92
<b>QCM</b>	Catalyzed deposition of gold	Affinity interaction	~ 1 fM	~ 3 h	93
	DNA hybridization on a nanoparticle-covered QCM surface	Thiol-modified oligonucleotide	0.1 fM	~ 4 h	94, 95
	Adsorption of a probe-target-nanoamplicon complex	Thiol-modified tetramers	0.17 aM	9.5 min.	96
<b>SPR</b>	Sandwich hybridization, PNA probes	Affinity interaction	1 fM	1.5 h	39
			41 zM		40